

***Arabidopsis* ROOT UVB SENSITIVE2/WEAK AUXIN RESPONSE1 Is Required for Polar Auxin Transport**

L. Ge,^a W. Peer,^b S. Robert,^c R. Swarup,^d S. Ye,^e M. Prigge,^a J.D. Cohen,^e J. Friml,^c A. Murphy,^b D. Tang,^f and M. Estelle^{a,1}

^a Cell and Developmental Biology, University of California San Diego, La Jolla, California 92093-0116

^b Department of Horticulture and Landscape Architecture, Purdue University, West Lafayette, Indiana 47907

^c Department of Plant Systems Biology, Flanders Institute for Biotechnology, and Department of Plant Biotechnology and Genetics, Ghent University, 9053 Ghent, Belgium

^d School of Biosciences and Centre for Plant Integrative Biology, University of Nottingham, Nottingham LE12 5RD, United Kingdom

^e Department of Horticultural Science and Microbial and Plant Genomics Institute, University of Minnesota, St. Paul, Minnesota 55108

^f State Key Laboratory of Plant Cell and Chromosome Engineering, Institute of Genetics and Developmental Biology, Chinese Academy of Sciences, Beijing 100101, China

Auxin is an essential phytohormone that regulates many aspects of plant development. To identify new genes that function in auxin signaling, we performed a genetic screen for *Arabidopsis thaliana* mutants with an alteration in the expression of the auxin-responsive reporter *DR5rev:GFP* (for green fluorescent protein). One of the mutants recovered in this screen, called *weak auxin response1* (*wxr1*), has a defect in auxin response and exhibits a variety of auxin-related growth defects in the root. Polar auxin transport is reduced in *wxr1* seedlings, resulting in auxin accumulation in the hypocotyl and cotyledons and a reduction in auxin levels in the root apex. In addition, the levels of the PIN auxin transport proteins are reduced in the *wxr1* root. We also show that *WXR1* is *ROOT UV-B SENSITIVE2* (*RUS2*), a member of the broadly conserved DUF647 domain protein family found in diverse eukaryotic organisms. Our data indicate that *RUS2/WXR1* is required for auxin transport and to maintain the normal levels of PIN proteins in the root.

INTRODUCTION

The plant hormone auxin regulates essential aspects of plant growth and development, including embryo patterning, root and shoot elongation, tropic response, and vascular differentiation (Davies, 1995). Recent studies indicate that auxin controls development through a complex regulatory network involving auxin biosynthesis, transport, and perception (Benjamins and Scheres, 2008). In both the root and shoot, these processes contribute to the formation of an auxin concentration gradient required for patterning of developing tissues. Formation and maintenance of auxin gradients is dependent on polar cell-to-cell auxin transport mediated by special transporter proteins, including the auxin influx carriers AUX/LAX, the efflux facilitators PIN FORMED (PIN), and several ABCB proteins (Gälweiler et al., 1998; Marchant et al., 1999; Noh et al., 2001, 2003; Geisler et al., 2005; Bandyopadhyay et al., 2007; Petrasek and Friml, 2009;

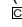
Robert and Friml, 2009). Moreover, modeling studies suggest that polar auxin transport is necessary to generate an auxin maximum and concentration gradient in the root tip (Grieneisen et al., 2007; Robert and Friml, 2009).

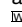
The patterns of expression and cellular localization of the AUX1 and PIN proteins are key to their function. For example, in *Arabidopsis thaliana* roots, AUX1 is expressed in stele, columella, epidermis, and lateral root cap cells and is polarly localized on the apical side of the protophloem cells (Swarup et al., 2001). The cellular localizations of PIN proteins vary depending on the protein and cell type. In general, however, the localization of the auxin efflux carriers correlates with and determines the direction of auxin transport (Gälweiler et al., 1998; Friml et al., 2002a, 2002b; Wisniewska et al., 2006).

Localization of the PIN proteins is a dynamic process that responds rapidly to physiological and environmental changes (Paciorek et al., 2005; Kleine-Vehn et al., 2008; Laxmi et al., 2008; Pan et al., 2009; Petrasek and Friml, 2009; Robert and Friml, 2009). PIN1 and related proteins are constitutively internalized by clathrin-dependent endocytosis and relocalized to the plasma membrane by ARF-GEF-dependent (guanine-nucleotide exchange factors for ADP-ribosylation factor GTPase) recycling (Geldner et al., 2001; Dhonukshe et al., 2007). Studies using yellow fluorescent protein (YFP)-tagged PIN1 and inducible PIN1 proteins indicate that PIN polar localization involves a two-step mechanism: the newly synthesized PIN proteins are localized to

¹ Address correspondence to mestelle@ucsd.edu.

The author responsible for distribution of materials integral to the findings presented in this article in accordance with the policy described in the Instructions for Authors (www.plantcell.org) is: M. Estelle (mestelle@ucsd.edu).

 Some figures in this article are displayed in color online but in black and white in the print edition.

 Online version contains Web-only data.

www.plantcell.org/cgi/doi/10.1105/tpc.110.074195

the plasma membrane nonpolarly, and their polar localization is mediated by the Rab5 GTPases (named ARA7 and RHA1 in *Arabidopsis*) endosome pathway (Dhonukshe et al., 2008). ARA7 and the putative retromer complex components SORTING NEXIN1 and VACUOLAR PROTEIN SORTING29, which are localized in late endosomes in the plant (Jaillais et al., 2006, 2007), are thought to be necessary for retrieval of PIN2 from late endosomes and thus prevent it from being internalized into lytic vacuoles (Abas et al., 2006; Kleine-Vehn et al., 2008). Moreover, this vacuolar internalization pathway mediates aspects of the response to gravity stimulation. A gravity stimulus increases the amount of PIN2 internalized into vacuoles on the upper side of epidermal cells after reorientation of root growth (Kleine-Vehn et al., 2008; Pan et al., 2009).

Once auxin is transported to a target tissue, auxin interacts with the TIR1/AFB auxin receptors and promotes degradation of the AUXIN/INDOLE-3-ACETIC ACID (Aux/IAA) proteins to allow ARF-dependent regulation of transcription (Dharmasiri et al., 2005a; Kepinski and Leyser, 2005). Genetic studies of the *TIR1/AFB*, *Aux/IAA*, and *ARF* genes indicate that auxin is required for establishment of the root meristem and postembryonic root growth. Because previous genetic screens for auxin-resistant mutants involved examination of auxin response in the seedling root, it is possible that mutants with severe defects in auxin response were not recovered. In an attempt to circumvent this problem, we used the well-characterized auxin reporter *DR5rev:GFP* (for green fluorescent protein) to screen for mutants with altered auxin response. We isolated several previously uncharacterized mutants with short primary roots and auxin response defects. Here, we report the isolation and characterization of *weak auxin response1 (wxr1)*, an allele of the *ROOT UV-B SENSITIVE2 (RUS2)* gene (Leasure et al., 2009). *RUS2/WXR1* encodes a protein belonging to the DUF647 family (for Domain of Unknown Function 647). In this study, we show that the *wxr1* mutant has reduced levels of the auxin efflux proteins PIN1, PIN2, and PIN7. This defect results in a reduction in polar auxin transport and, as a consequence, altered auxin responses.

RESULTS

The *wxr1* Mutant Has Short Roots and an Auxin Response Defect

To discover new genes involved in auxin signaling, we mutagenized seeds carrying the auxin-responsive reporter *DR5rev:GFP* with ethyl methanesulfonate and screened M2 plants on medium containing 75 nM 2,4-D. Five-day-old seedlings with reduced GFP signal in the root were identified and transferred to medium without auxin for further analysis. Eight single gene recessive mutants were ultimately recovered, called *wxr* mutants.

The *wxr1* mutant displays severe defects in root development and slight defects in leaf and inflorescence development (Figure 1). To characterize the *wxr1* phenotype in more detail, M3 plants were backcrossed to *Columbia-0 (Col-0) (DR5rev:GFP)* plants three times. When 5-d-old seedlings were placed on 75 nM 2,4-D medium for 12 h, wild-type plants carrying *DR5rev:GFP*

display an increase in GFP signal in the root tip, whereas *wxr1* plants do not exhibit an obvious change (Figures 1B and 1D). A similar result was obtained when *wxr1* plants were tested on medium containing IAA or 1-naphthalene acetic acid (see Supplemental Figure 1 online).

When grown using our typical growth conditions (continuous white light, 80 to $\sim 90 \mu\text{E m}^{-2} \text{ s}^{-1}$, 22°C), the young *wxr1* seedlings accumulate anthocyanin in the cotyledons and hypocotyls (Figure 1F) and primary root elongation is dramatically reduced. The roots of wild-type seedlings were 5.5 ± 0.5 cm (mean \pm SE, $n = 16$) after 7 d on ATS medium, whereas *wxr1* roots were only 0.5 ± 0.1 cm (mean \pm SE, $n = 15$) (Figure 1G). Furthermore, root hairs on mutant seedlings initiate but do not elongate (Figure 1I). Lugol staining revealed that 7-d-old mutant roots had fewer columella cells than did wild-type roots and that those cells were disorganized (Figure 1J). The cell pattern was irregular in the *wxr1* root tip, and the meristem region was much smaller (Figures 2A and 2B). Five-day-old wild-type plants had 49 ± 4.5 (mean \pm SE, $n = 10$) meristem cortex cells, whereas *wxr1* plants had 22 ± 2 meristem cortex cells (mean \pm SE, $n = 10$, *t* test, $P < 0.005$). The rosette leaves of 3-week-old *wxr1* mutants were smaller than those of wild-type plants (Figure 1H), and at 5 weeks, mutant plants displayed a slight decrease in apical dominance. Shoot number, including primary and axillary shoots, was 3.88 ± 0.60 in *wxr1* and 1.63 ± 0.99 in wild-type plants (mean \pm SE, $n = 50$, *t* test, $P < 0.005$). These data indicate that the *wxr1* mutation affects mainly root growth and has a smaller effect on development of the rosette and inflorescence.

During the course of our studies, we found that *wxr1* plants are hypersensitive to both light and temperature. When grown at the elevated temperature of 29°C in white light, the meristem cortex cell number of *wxr1* plants did not change (21 ± 3.1 , mean \pm SE, $n = 10$), but primary root elongation increased dramatically (Figures 2C and 2E). When *wxr1* plants were grown at lower light levels ($\sim 50 \mu\text{E m}^{-2} \text{ s}^{-1}$, 24 h/day, 22°C, yellow filters), both primary root length and meristem cell number were increased relative to the wild type (Figures 2D and 2E). To determine if this effect was specific for yellow light, we also grew seedlings in low levels of far-red, red, and blue light, as well as in dark conditions. In each case, the effect of *wxr1* on root growth was reduced relative to that in high levels of white light, indicating that *wxr1* roots were responding to reduced light intensity rather than to a specific wavelength (see Supplemental Figure 2 online). In yellow light and high temperature ($\sim 50 \mu\text{E m}^{-2} \text{ s}^{-1}$, 24 h/day, 29°C), *wxr1* root elongation was further stimulated (Figure 2E). High temperature has been shown to cause an increase in auxin levels in seedlings, and light affects both local auxin levels as well as auxin transport (Gray et al., 1998; Gil et al., 2001; Tao et al., 2008). Thus, it is possible that increased temperature and reduced light result in increased levels of endogenous auxin and that this change partially restores root growth. To investigate this possibility, we used the *DR5rev:GFP* reporter. Surprisingly, we found that GFP levels were decreased in both wild-type and *wxr1* roots grown at low light ($\sim 30 \mu\text{E m}^{-2} \text{ s}^{-1}$, 22°C) (Figures 2F, 2G, 2J, and 2K). However, GFP levels were increased at elevated temperature in both genotypes (Figures 2H and 2L). Furthermore, this increase was even more dramatic in roots grown in low light and high temperature, suggesting a

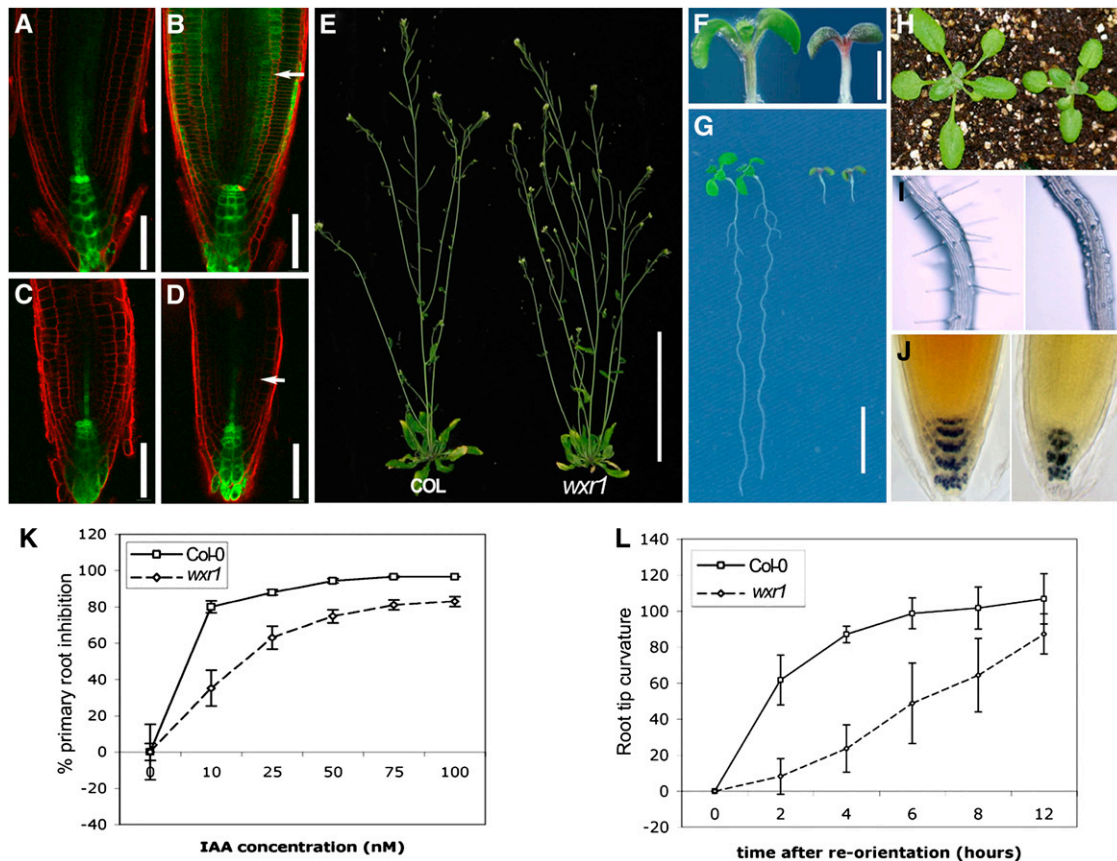


Figure 1. Phenotype of the *wxr1* Mutant.

(A) to (D) *DR5rev:GFP* expression in 5-d-old *wxr1* and wild-type seedlings. Before auxin treatment, the GFP signal (green) is similar in wild-type (A) and in *wxr1* (C) root tips. Treatment with 75 nM 2,4-D for 12 h results in a strong increase in GFP signal in the wild type (B) but not in the mutant (D). Roots were stained with propidium iodide before observation. Arrows indicate cortical cells. Bars = 50 μ m; $n \geq 30$.

(E) Five-week-old *wxr1* plants (right) display decreased apical dominance compared with wild-type plants (left). Bar = 10 cm.

(F) 7-day-old *wxr1* (right) seedlings accumulate more pigment in cotyledons and hypocotyls than does the wild type (left). Bar = 1 mm.

(G) The growth of *wxr1* roots (right, 7 d old) is dramatically reduced. Bar = 1 cm.

(H) The rosette leaves and petioles of 3-week-old *wxr1* plants (right) are smaller than the wild type (left).

(I) *wxr1* root hairs (right) exhibit reduced root hair elongation compared with the wild type (left).

(J) Wild-type (left) and *wxr1* roots (7 d after germination) stained with Lugol's solution.

(K) Effect of auxin on root elongation in wild-type and *wxr1* seedlings grown in yellow light. Bars represent SE, $n = 14$

(L) The roots of *wxr1* seedlings exhibit a reduced response to gravity after 90° reorientation on half-strength MS medium in the dark. Error bars represent SE, $n = 25$

synergism between these two environmental conditions (Figures 2I and 2M).

Since primary root elongation is reduced so dramatically under our standard light conditions, it was difficult to measure changes in primary root length in *wxr1*. As an alternative, we analyzed root growth under yellow light. The results in Figures 1K and 1L show that *wxr1* seedlings have reduced responses to IAA and gravity, consistent with a defect in auxin response. To characterize further the gravitropic defect, we also constructed double mutants with *axr2-1*, *aux1-7*, and *abcb1*. Each of these mutants is affected in gravitropism due to a defect in auxin signaling or transport (Pickett et al., 1990; Wilson et al., 1990; Noh et al., 2001). The double mutants were all more severely affected than

were the corresponding single mutants (see Supplemental Figure 3 online).

The *wxr1* Mutant Exhibits a Synergistic Interaction with Mutations in Auxin Receptor Genes

To examine the function of WXR1 in auxin signaling, we introduced *wxr1* into *tir1-1*, *tir1-1 afb3-1*, and *tir1-1 afb2-1 afb3-1* mutants defective in auxin perception (Dharmasiri et al., 2005b). The seedling roots of *tir1-1* and *tir1-1 afb3-1* were similar to those of wild-type plants except that they had fewer lateral roots (Dharmasiri et al., 2005b). By contrast, 24% of *wxr1 tir1-1 afb3-1* seedlings ($n = 147$) did not develop a root and died on the plates.

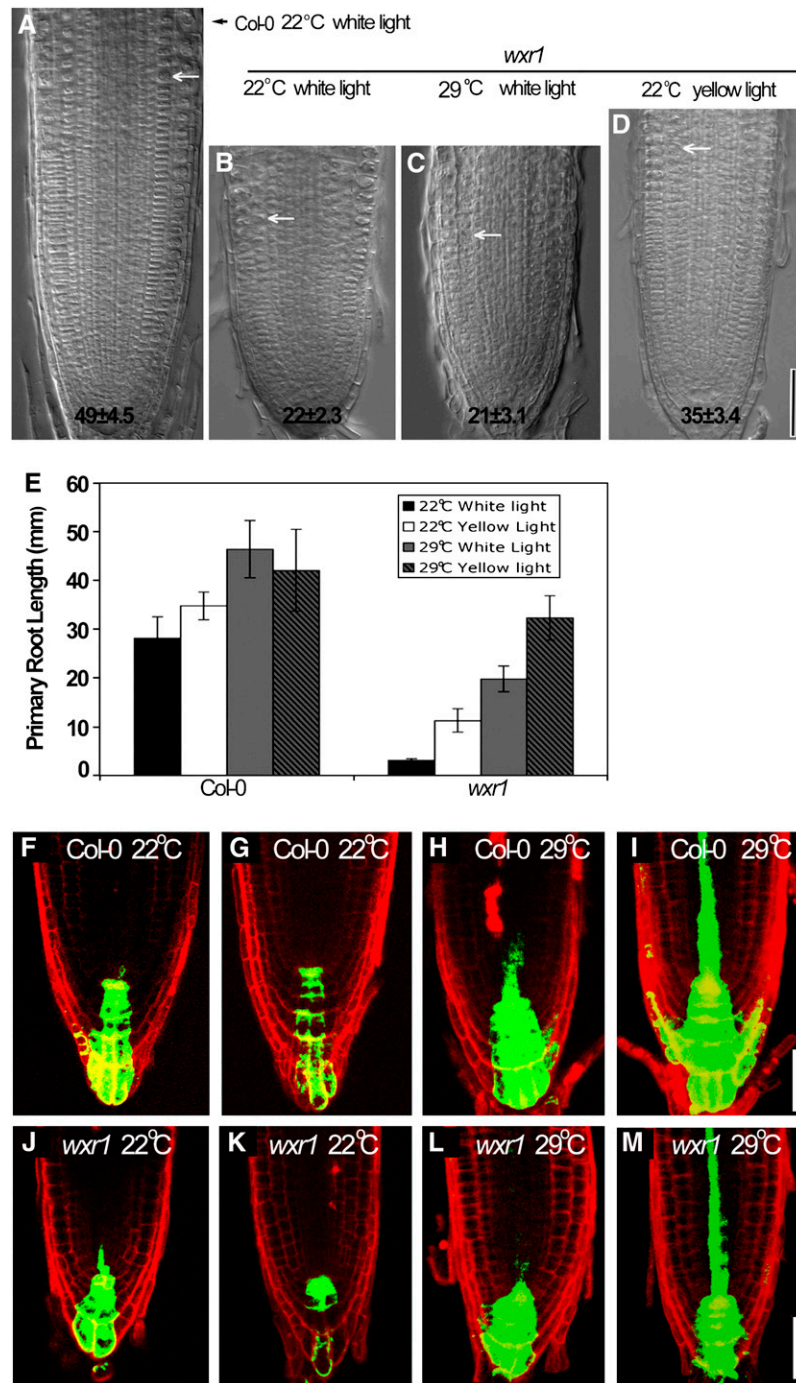


Figure 2. The *wxr1* Mutation Causes Short Primary Roots and Root Meristem Cell Proliferation Defects.

(A) to (D) Five-day-old wild-type and *wxr1* seedlings grown under indicated light and temperature conditions. Arrows show the boundary between the meristem zone and elongation zone. Numbers indicate cortical cell number in the meristem zone (mean \pm SE). Bar = 50 μ m.

(E) Elongation of 7-d-old *wxr1* roots was rescued by low intensity light or high temperature. Error bars represent SE, $n = 30$.

(F) to (M) *DR5rev:GFP* expression in 5 d after germination *wxr1* and wild-type seedlings grown at indicated temperature. Seedlings in (F), (H), (J), and (L) were grown in 80 to 90 μ E $m^{-2} s^{-1}$, while those in (G), (I), (K), and (M) were grown at 30 μ E $m^{-2} s^{-1}$. Bars = 50 μ m.

Similarly, introduction of *wxr1* into *tir1-1 afb2-1 afb3-1* had a dramatic effect on seedling phenotype. Greater than 50% of *tir1-1 afb2-1 afb3-1* survived beyond the seedling stage, whereas <12% of *wxr1 tir1-1 afb2-1 afb3-1* seedlings survived ($n = 176$) and these had much more severely affected primary roots than those of *wxr1*. The rosettes of 3-week-old *wxr1 tir1-1 afb2-1 afb3-1* plants had extremely small rosette leaves compared with those of *tir1-1 afb2-1 afb3-1* and *wxr1* plants and exhibited an early yellowing phenotype (Figures 3A to 3F). The inflorescences of *wxr1 tir1-1 afb2-1 afb3-1* were also very small, whereas those of *wxr1 tir1-1 afb3-1* were similar to those of *tir1-1 afb2-1 afb3-1* plants after flowering (Figure 3G). These results confirm that *wxr1* is deficient in auxin-related processes.

Aux/IAA Degradation in the *wxr1* Mutant

To investigate further the effects of WXR1 on auxin response, the *HS:AXR3NT-GUS* (for β -glucuronidase) transgene was intro-

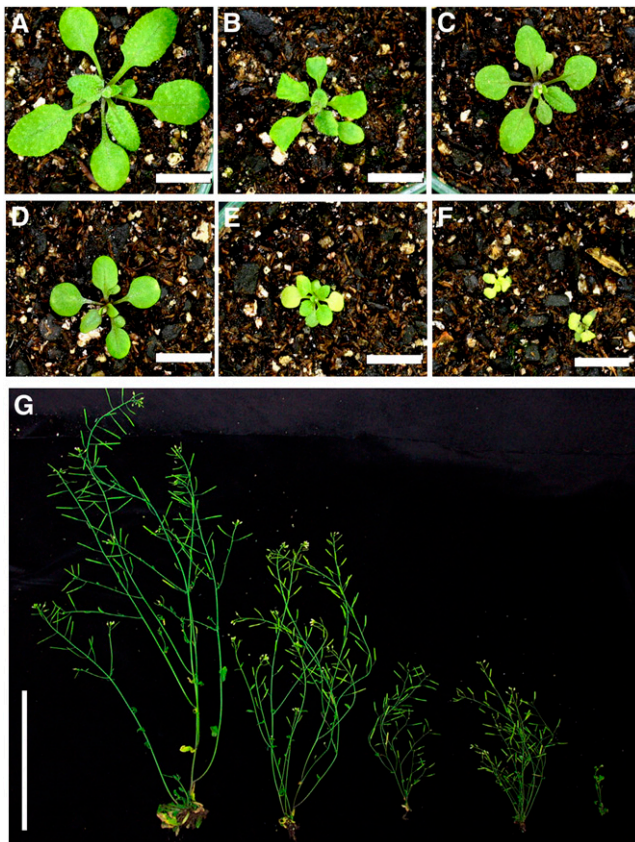


Figure 3. The *wxr1* Mutation Displays a Synergistic Interaction with the *tir1-1 afb2-1 afb3-1* Mutant.

(A) to (F) Three-week-old *wxr1 tir1-1 afb2-1 afb3-1* plants have extremely small curled-down rosette leaves. The plants from (A) to (F) are *Col-0*, *tir1-1 afb2-1 afb3-1*, *wxr1*, *wxr1 tir1-1*, *wxr1 tir1-1 afb3-1*, and *wxr1 tir1-1 afb2-1 afb3-1*, respectively. Bars = 1 cm.

(G) Five-week-old *wxr1 tir1-1 afb2-1 afb3-1* plants produce extremely short inflorescences. Plants from left to right are *Col-0*, *wxr1*, *tir1-1 afb2-1 afb3-1*, *wxr1 tir1-1 afb3-1*, and *wxr1 tir1-1 afb2-1 afb3-1*, respectively. Bar = 10 cm.

duced into *wxr1* mutant plants. AXR3NT-GUS is a substrate for SCF^{TIR1/AFB}s and provides a useful tool to assess SCF^{TIR1/AFB} function in the plant (Gray et al., 2001; Dharmasiri et al., 2005b). Seven-day-old wild-type and *wxr1* seedlings carrying the *HS:AXR3NT-GUS* construct were heat shocked for 2 h at 37°C in the dark. Seedlings were transferred to plates with or without IAA at 22°C and stained for GUS at time intervals. The roots of *wxr1* seedlings accumulated much more AXR3NT-GUS than did those of wild-type plants following heat shock (Figure 4A). However, upon auxin treatment, GUS staining rapidly decreased in both wild-type and mutant roots. Measurement of GUS activity by fluorescent β -galactosidase methylumbelliferylglucuronide (MUG) assay showed that AXR3NT-GUS was degraded at a similar rate in both wild-type and *wxr1* plants (Figure 4H). These results indicate that the auxin-resistant aspects of the *wxr1* phenotype cannot be explained by a reduction in SCF^{TIR1/AFB}-dependent degradation of Aux/IAA proteins. However, AXR3NT-GUS accumulation was reduced in the cotyledons and hypocotyls of *wxr1* plants compared with the wild type, suggesting that degradation of the protein was accelerated in the aerial parts of the *wxr1* mutant (Figures 4B and 4C).

Auxin Accumulates in the Shoots of *wxr1* Plants

To explore how auxin distribution is affected in the *wxr1* mutants, *BA3:GUS*, a sensitive auxin-responsive reporter, was introduced into *wxr1* plants (Oono et al., 1998). As for the *DR5rev:GFP* reporter, GUS staining was weaker in auxin-treated mutant roots compared with the wild type (Figures 4D and 4E). By contrast, GUS staining was stronger in the leaves and hypocotyls of *wxr1* plants than in those of the wild type (Figures 4F and 4G).

One interpretation of these results is that *wxr1* affects transport of IAA from sites of production in the shoot to the root. To assess this possibility, we directly measured free IAA levels in aerial tissues of wild-type and mutant seedlings. The results show that IAA levels are increased in the mutant compared with the wild type (Figure 4I). To test our hypothesis that the *wxr1* mutant is deficient in auxin transport, we directly measured transport in seedlings using ³H-IAA. The results in Figure 4J show that transport of applied IAA out of the hypocotyl into the root is reduced in *wxr1* plants. In addition, we found a reduction in accumulation of IAA in the root tip (Figure 4K). Together, these results indicate that *wxr1* interferes with IAA distribution in the *Arabidopsis* seedling by reducing auxin transport.

The *wxr1* Mutant Has Reduced Levels of PIN and AUX1 Protein in the Plasma Membrane

Auxin efflux carriers of the PIN family and the auxin influx carrier AUX1 both contribute to polar auxin transport. Because *wxr1* plants are deficient in auxin transport, we next examined the levels and distribution of several PIN proteins and AUX1 in the mutant. Localization of AUX1 using a *AUX1:AUX1-YFP* line revealed slightly reduced AUX1 levels in the *wxr1* background (Figures 5G and 5H) (Swarup et al., 2004). By contrast, in situ immunodetection using anti-PIN1 and anti-PIN2 antisera revealed that the levels of these two proteins were dramatically decreased in 3- to 4-d-old *wxr1* roots compared with the wild

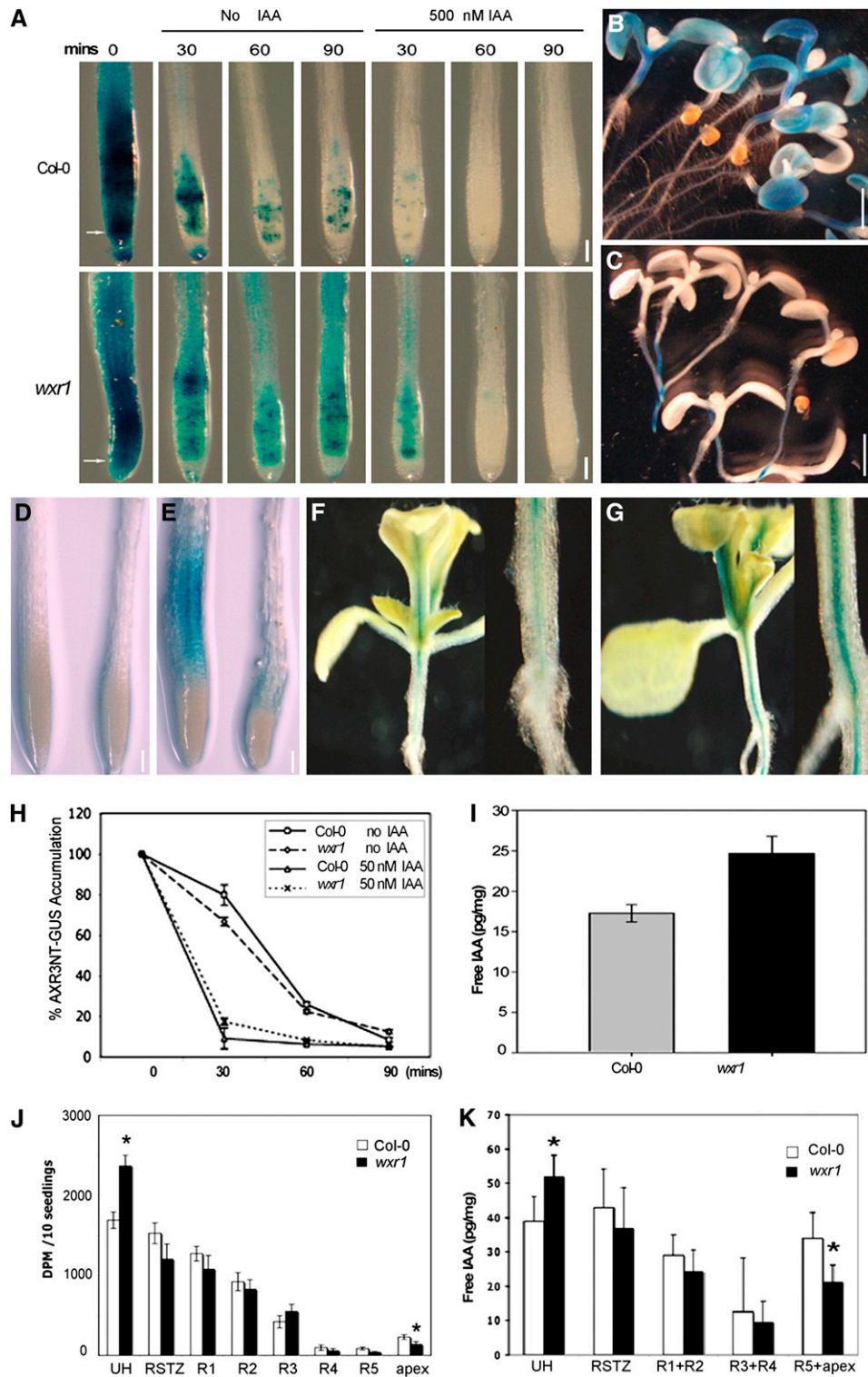


Figure 4. Auxin Distribution Is Altered in the *wxr1* Mutant.

(A) GUS staining of *HS:AXR3NT-GUS* lines after heat shock in the absence and presence of 500 nM IAA. AXRNT-GUS levels were higher in the untreated mutant than in the wild type but decreased upon auxin treatment.

(B) and **(C)** AXR3NT-GUS staining in wild-type **(B)** and *wxr1* cotyledons **(C)** after a 2-h heat shock and 20-min recovery at room temperature.

(D) and **(E)** Expression of *BA3:GUS* in *Col-0* and *wxr1* roots after 24 h treatment with buffer **(D)** or 100 nM IAA **(E)**. In each panel, *Col-0* root is on the left

type (Figures 5A to 5D). To examine PIN7 levels, we introduced *PIN7:PIN7-GFP* into *wxr1* plants. As for the other PIN proteins, the level of PIN7-GFP was clearly reduced in 5-d-old *wxr1* root tips (Figures 5E and 5F). To determine if these differences reflect changes in transcription, the transcript levels of *AUX1*, *PIN1*, *PIN2*, and *PIN7* were examined in 5-d-old *wxr1* seedlings by quantitative RT-PCR. The results indicate that transcript levels are similar in *Col-0* and *wxr1* plants, suggesting that the effect on protein level is posttranscriptional (Figure 5I).

To determine if *wxr1* has a specific effect on proteins involved in auxin transport, we crossed transgenes expressing the marker proteins VHA-a1-GFP (trans-Golgi network), GNOM-GFP (recycling endosomes), or ARA7-GFP (prevacuolar compartment) into mutant plants (Geldner et al., 2003; Lee et al., 2004; Dettmer et al., 2006). Surprisingly, the levels of these proteins were also reduced in *wxr1*, indicating that the effects of the mutation are not specific to auxin transport proteins (Figures 5J to 5O). By contrast, the levels of the tonoplast marker *vac-yb* was increased in *wxr1* roots (see Supplemental Figure 4 online).

If the *wxr1* phenotype is related to reduced PIN levels, it is possible that more PIN protein may partially suppress the phenotype. To test this possibility, we crossed *PIN1:PIN1-GFP* and *PIN2:PIN2-GFP* into *wxr1* plants. Plants homozygous for these transgenes, carrying four copies of the *PIN1* and *PIN2* genes, respectively, displayed increased root elongation compared with *wxr1* ($n \geq 14$, t test, $P < 0.001$), indicating partial rescue of the mutant phenotype (Figure 6G). In addition, the root hairs of *wxr1 PIN1:PIN1-GFP* and *wxr1 PIN2:PIN2-GFP* were nearly the same as those of the wild type (Figures 6A to 6F).

WXR1 Is a Member of the DUF647 Family and Is Expressed in All Plant Organs

To map the *wxr1* mutation, genomic DNA was isolated from 438 F2 plants generated in a cross of *wxr1 (Col-0)* with *Landsberg erecta*. Homozygous *wxr1* plants were identified based on the short-root phenotype. The *wxr1* mutation was first mapped between simple sequence length polymorphism markers *nga168* and *nga1126*. Additional fine mapping placed the mutation in a 90-kb region containing 42 genes. The coding regions of all 42 genes were sequenced. A single mutation was found in *At2g31190* that results in the substitution of Ser-105 with Leu. *At2g31190* is identical to the previously identified *RUS2* gene, implicated in response to UV light (Leasure et al., 2009). Ser-105 is located in a highly conserved motif, TQXLL, present in most members of this family (see Supplemental Figure 5A online).

DUF647 protein family members are encoded by most of the eukaryotic genomes sequenced to date (see Supplemental Data Set 1 online). Phylogenetic analysis indicates that several subfamilies diverged very early in eukaryotic evolution, but different eukaryotic lineages exhibit different propensities to retain members of the different DUF647 clades (see Supplemental Figure 6 online). Whereas plants and red algae have retained multiple lineages of DUF647 proteins, most animals and fungi have only retained a single DUF647 protein, and several species, including yeasts and nematodes, lack DUF647 proteins. Thus, DUF647 proteins are probably involved in a process common to most, but not all, eukaryotes.

The *At2g31190* cDNA was isolated by RT-PCR and used to generate C-terminal GFP and GUS fusions under control of the cauliflower mosaic virus 35S promoter or the *WXR1* promoter and introduced into *wxr1* plants. Two *WXR1:WXR1-GFP*, four *35S:WXR1-GFP*, and eight *35S:WXR1-GUS* transgenic lines were analyzed (see Supplemental Figure 5B online). Root growth was partially restored in each line. However, the *WXR1-GFP* proteins were much more effective in rescuing the mutant phenotype than the *WXR1-GUS* line, perhaps because of the large size of the GUS protein. Overall, these results confirm that *At2g31190* is *WXR1*.

To analyze expression of the *WXR1* gene, we generated a *WXR1:WXR1-GUS* construct in which the same *WXR1* genomic DNA sequence of *WXR1:WXR1-GFP* was fused in frame with the *GUS* reporter gene and introduced into *wxr1* plants. GUS staining revealed that the transgene is active in most plant organs, including cotyledons, hypocotyls, roots, stems, flowers, and leaves (see Supplemental Figures 7A to 7D online). In particular, root tips, vascular tissues of all organs, and lateral root primordia showed strong GUS staining (see Supplemental Figures 7A to 7E online). Strong staining was also observed in root pericycle cells and lateral root primordia, suggesting that *WXR1* may play a role in lateral root initiation, perhaps through its effects on auxin transport.

WXR1 Is Present in Plastids

Several proteomic studies suggest that *WXR1* is localized to the chloroplast envelope (Ferro et al., 2003; Dunkley et al., 2006). To investigate this possibility further, we introduced *WXR1:WXR1-GFP* into *wxr1* as well as into *Col-0* plants expressing *pt-rb* and *px-rb* proteins, mCherry-based markers for the plastid and peroxisome, respectively (Nelson et al., 2007). The data in Figures 7A and 7B show that *WXR1-GFP* colocalizes with *pt-rb* but not *px-rb*, indicating that *WXR1* is localized to the plastid. The distribution of *WXR1-GFP* was also examined in hypocotyls and

Figure 4. (continued).

and the *wxr1* root on the right.

(F) and (G) Expression of *BA3:GUS* in shoots of *Col-0* (F) and *wxr1* plants (G). The image on the right of each panel is a close up of the hypocotyl.

(H) GUS activity in the root tips of seedlings from (A) measured by MUG assay. Error bars represent SE, $n = 30$.

(I) The levels of IAA are increased in the shoots of *wxr1* plants compared with the wild type. Error bars represent SD, $n = 10$.

(J) Transport of ^3H -IAA was reduced in *wxr1* seedlings. UH, upper hypocotyl; RSTZ, root shoot transition zone; apex, root apex. The asterisks indicate significant differences between wild-type and mutant values based on Student's t test, $P < 0.05$. Error bars represent SE, $n = 10$.

(K) IAA levels in segments as described for (J). Error bars represent SE, $n = 3$.

Bars = 100 μm in (A), (D), and (E) and 1 mm in (B) and (C).

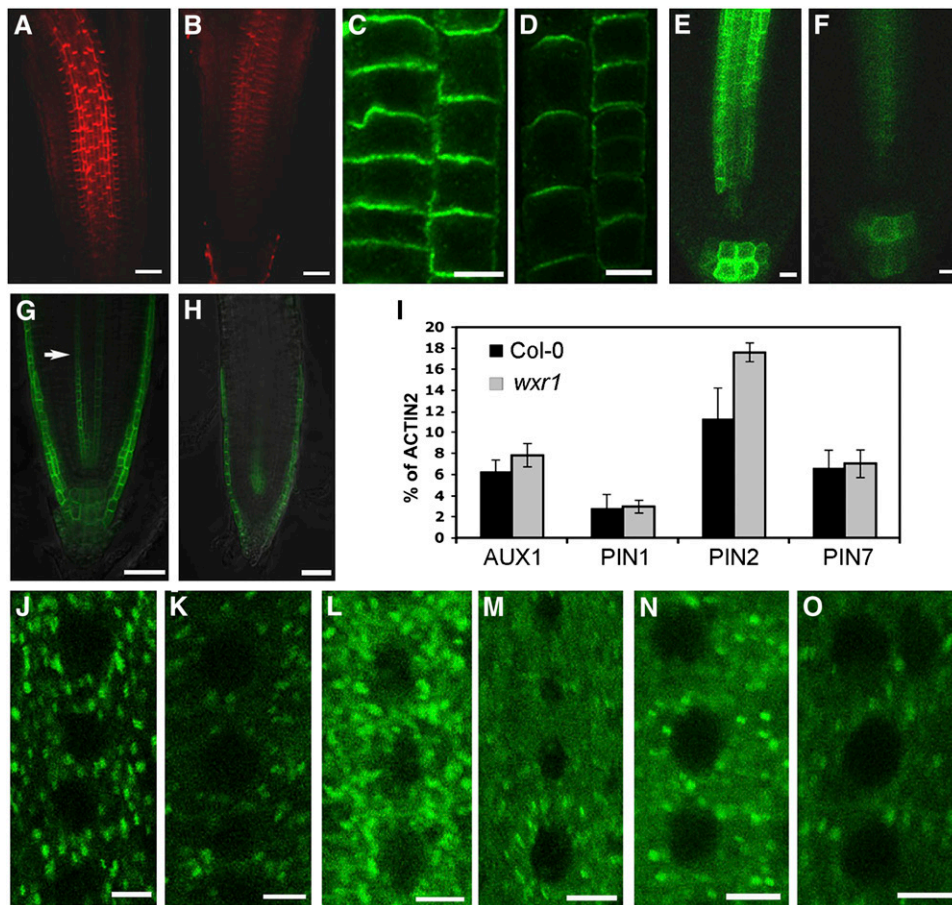


Figure 5. The Levels of Auxin Transport Carriers Are Reduced in *wxr1* Plants.

(A) to (H) The levels of PIN and AUX1 proteins are reduced in *wxr1* plants. Each experiment was repeated at least three times with at least 30 roots observed for each treatment.

(A) and (B) PIN1 visualized with anti-PIN1 antibody in the wild type (A) and *wxr1* (B). Bars = 50 μ m.

(C) and (D) PIN2 visualized with anti-PIN2 antibody in the wild type (C) and *wxr1* (D); epidermal cells on the left and cortical cells on the right of each panel. Bars = 10 μ m.

(E) and (F) PIN7::PIN7-GFP in wild-type (E) and *wxr1* (F) roots. Bars = 10 μ m.

(G) and (H) AUX1::AUX1-YFP in wild-type (G) and *wxr1* (H) seedlings (arrow indicates protophloem cells). Bars = 50 μ m.

(I) AUX1, PIN1, PIN2, and PIN7 transcript levels were assessed by real-time RT-PCR. ACT2 was used as a control.

(J) to (O) Comparison of VHA- α 1-GFP (J) and (K), GN-GFP (L) and (M), and ARA-7-GFP (N) and (O) levels in root epidermal cells of wild-type (J, L, and N) and *wxr1* (K, M, and O) plants. Bars = 5 μ m.

young rosette leaves. In this case, chloroplasts were visualized by autofluorescence. In both tissues, WXR1-GFP is associated with the chloroplast, confirming that the protein is plastid localized (Figures 7C and 7D).

Removal of UV-B Light Does Not Restore the *wxr1* Phenotype

Previous studies of the *rus2/wxr1* and *rus1* mutants suggested that the mutant phenotype is primarily the result of hypersensitivity to very-low-fluence-rate UV-B (Tong et al., 2008; Leasure et al., 2009). To explore this possibility further with the *wxr1* mutant, we examined the response of seedlings to various growth conditions. To test the effects of UV light on root growth,

we compared seedlings grown in dark conditions, white light, or white light passing through a UV filter that removes essentially all UV-B. Our results show that dark conditions increase root growth in *wxr1* seedlings but do not restore it to wild-type levels (see Supplemental Figure 8 online). By contrast, the removal of UV-B light resulted in only a modest stimulation of root growth in both wild-type and *wxr1* seedlings. These results suggest that factors other than UV light contribute to the *wxr1* phenotype.

DISCUSSION

Auxin has an essential role in many plant growth processes, including establishment of the root meristem during

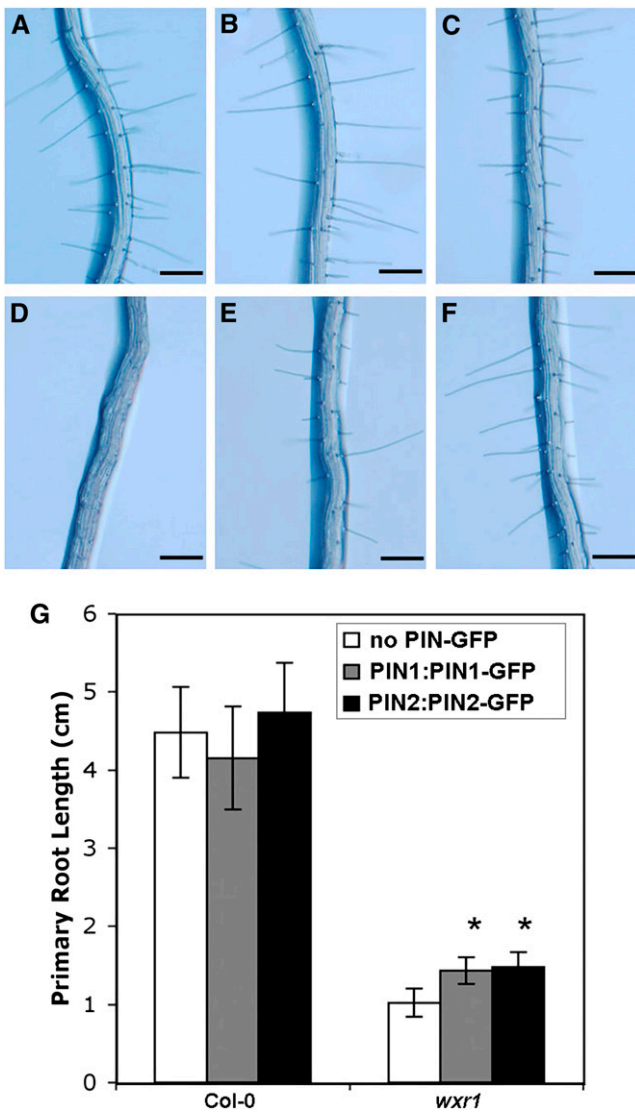


Figure 6. Increased Expression of *PIN1* and *PIN2* Partially Rescues Aspects of the *wxr1* Phenotype.

(A) to (F) Root hairs of *Col-0* (A), *PIN1:PIN1-GFP* (B), *PIN2:PIN2-GFP* (C), *wxr1* (D), *wxr1 PIN1:PIN1-GFP* (E), and *wxr1 PIN2:PIN2-GFP* (F); $n = 25$. Bars = 200 μm .

(G) Root length is increased in 8-d-old *PIN1:PIN1-GFP wxr1* and *PIN2:PIN2-GFP wxr1* compared with *wxr1*. Bars represent SE; $n \geq 14$, t test, $P < 0.001$.

[See online article for color version of this figure.]

embryogenesis subsequent patterning of the meristem, and other aspects of root development (Sabatini et al., 1999). In fact, many genes involved in auxin signaling have been identified in screens for mutants that display auxin-resistant root growth (Mockaitis and Estelle, 2008). However, mutants with severe defects in auxin perception or response, such as *tir1afb2afb3* or *bd1*, either lack a root completely or produce a very short root and thus would not be recovered in a simple screen for auxin resistance (Hamann et al., 1999; Dharmasiri et al., 2005b). To identify new genes in

auxin signaling, we used the *DR5rev:GFP* reporter and concentrated on mutants with short roots. In this study, we focus on the role of *RUS2/WXR1* in auxin-regulated root development.

The *wxr1* mutant was isolated based on reduced expression of *DR5rev:GFP* in the root. In addition, we show that *WXR1* is required for a number of auxin-regulated processes, such as root hair and lateral root production, root gravitropism, and root meristem maintenance. In addition, we observe a synergistic interaction between *wxr1* and mutations in the *TIR1/AFB* family of auxin receptors, consistent with a role for *WXR1* in some aspect of auxin biology.

Although it is clear that expression of both *DR5rev:GFP* and *BA3:GUS* is reduced in the root tips of *wxr1* plants, these reductions, as well many aspects of the pleiotropic growth phenotype, are better explained by a reduction in auxin transport rather than response. In young seedlings, the cotyledons and developing leaves are the primary sites of auxin production. This auxin is transported through the hypocotyl into the root system where it supports root elongation and the formation of lateral roots. Transport assays indicate that IAA transport from the apex of the seedling is reduced in *wxr1* seedlings. Indeed, free IAA levels are increased in the aerial portion of mutant seedlings compared with the wild type but decreased in the root apex.

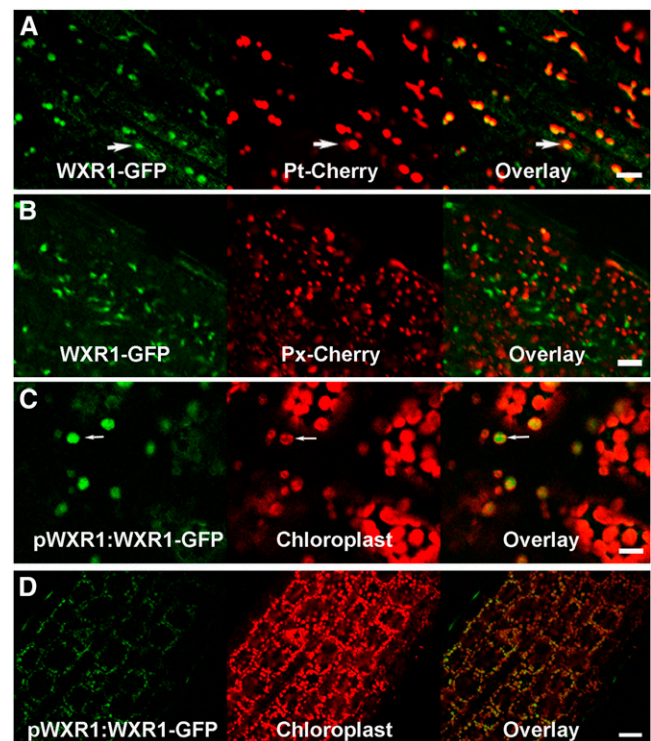


Figure 7. *WXR1* Localizes to Plastids.

(A) and (B) *WXR1-GFP* colocalizes with plastid marker Pt-Cherry in epidermal cells of wild-type roots (A) but not with the peroxisome marker Px-Cherry (B).

(C) and (D) *WXR1-GFP* colocalizes with autofluorescence of the chloroplast in *wxr1 WXR1:WXR1-GFP* leaves (C) and hypocotyls (D). Bars = 10 μm in (A) to (C) and 20 μm in (D).

However, it is important to note that WXR1 is unlikely to have a specific role in auxin transport, and some aspects of the phenotype are probably not related to auxin (see below).

Auxin transport is mediated by the AUX1/LAX influx carriers as well as the PIN and ABCB efflux carriers (Bandyopadhyay et al., 2007; Robert and Friml, 2009). The cellular localizations of both AUX1 and the PINs are dynamically regulated in a cell-type-specific manner. In the case of the PINs, localization occurs through a GNOM-dependent recycling pathway and is regulated by the PID kinase (Friml et al., 2004; Michniewicz et al., 2007; Kleine-Vehn et al., 2009; Sukumar et al., 2009; Zhang et al., 2010). AUX1 trafficking is not dependent on GNOM but does require an endoplasmic reticulum-localized protein called AXR4 (Dharmasiri et al., 2006; Kleine-Vehn et al., 2008). In our analysis, we find that WXR1 is required for normal accumulation of both PINs and AUX1 on the plasma membrane, providing a likely explanation for the observed decrease in auxin transport. In addition, we find that the levels of several other proteins involved in the endosomal pathway are reduced, including VHA- α 1-GFP, GNOM-GFP, and ARA7-GFP, indicating that the effect of *wxr1* is not restricted to auxin transport proteins.

WXR1 is a member of a family of six DUF647 proteins in *Arabidopsis* and identical to the previously identified RUS2 protein. Mutations in *RUS2* and another member of the family called *RUS1* result in hypersensitivity to UV light (Tong et al., 2008; Leasure et al., 2009). For a variety of reasons, it is unlikely that the primary function of RUS2/WXR1 is to mediate response to UV light. First, we were unable to demonstrate UV-hypersensitive root growth in *wxr1*. In fact, even in complete darkness, *wxr1* roots are shorter than wild-type roots. It is possible that this difference is related to the specific allele tested or an unknown difference in growth conditions. Second, we find that conditions that increase auxin movement into the root, such as elevated temperature or overexpression of PIN1, restore root growth in mutant roots. Third, the *wxr1* mutation enhances the strong embryonic phenotype of the receptor *tir1afb2afb3* mutants, indicating that WXR1 contributes to embryogenesis. It seems likely that both the defect in auxin transport/distribution and the UV hypersensitivity are consequences of a defect in cellular regulation, perhaps in protein trafficking. Until we obtain information on the biochemical function of the DUF647, this issue will remain unresolved.

Proteomic studies suggest that WXR1 is localized to the chloroplast envelope (Ferro et al., 2003; Dunkley et al., 2006). We confirmed this using a *WXR1-GFP* line. Because the biochemical function of RUS2/WXR1 and other members of the DUF647 family is unknown, there is no clear model for how the loss of a chloroplast-localized protein impacts the levels of proteins in other membranes. DUF647-containing proteins are present in other plants, as well as most animals and fungi, and in the future it will be interesting to determine if these proteins also function in endocytosis and protein trafficking.

METHODS

Plant Materials and Conditions

All *Arabidopsis thaliana* lines used in this article were generated in the *Col-0* ecotype with the exception of *afb2-1* and *afb3-1* lines, which are T-DNA

insertion lines in *Wassilewskija* ecotype. The transgenic plants *GN:GN-GFP*, *VHA- α 1-GFP*, and *ARA-7-GFP* (Geldner et al., 2003; Lee et al., 2004; Dettmer et al., 2006) were kindly provided by Gerd Jurgens. The *PIN1:PIN1-GFP*, *PIN2:PIN2-GFP*, *PIN7:PIN7-GFP*, *DR5rev:GFP*, and *AUX1:AUX1-YFP* have been described (Swarup et al., 2001; Benkova et al., 2003; Bliou et al., 2005). The *HS:AXR3NT-GUS wxr1* and *BA3:GUS wxr1* lines were made by crossing *war* plants to *HS:AXR3NT-GUS* and *BA3:GUS* plants (Oono et al., 1998; Gray et al., 2001). The *axr2-1*, *abcb1/pgp1*, and *aux1-7* mutants have been described (Pickett et al., 1990; Wilson et al., 1990; Geisler et al., 2005). Seedlings were grown in a growth chamber (80 to \sim 90 μ E/m²s measured by LI-185B Quantum/Radiometer/photometer [LI-COR], 24 h/day, 22°C) on ATS medium plates except where indicated (Lincoln et al., 1990). Yellow light (\sim 50 μ E/m²s measured by LI-185B Quantum/Radiometer/photometer; LI-COR) was produced using a medium yellow filter, 480 (Gamproducts). 1-naphthalene acetic acid, 2,4-D, and IAA treatment were performed by adding different auxins to half-strength Murashige and Skoog (MS) (1% sucrose and 0.8% agar) plates.

35S:*WXR1-GFP* and 35S:*WXR1-GUS* constructs were generated by introducing full length of *WXR1* from pENTR-D (Invitrogen) into *pMDC83* and *pMDC140* using the Gateway LR reaction kit (Invitrogen). *WXR1:WXR1-GFP* and *WXR1:WXR1-GUS* constructs were made by introducing *WXR1* genomic DNA sequence plus 2.0 kb upstream genomic DNA sequence into *pMDC107* and *pMDC163*. The primers (*WXR1CDS*, sense, 5'-CACCATGCAGTTTCTTCAGGAGAAGG-3', antisense, 5'-AGCAAATCTTGTCCTCCCGTGC-3'; *WXR1* genomic DNA with promoter, sense, 5'-CACCGGTCATGCAATCTCGCTTTTG-3', antisense, 5'-AGCAAATCTTGTCCTCCCGTGC-3') were synthesized by Invitrogen. pt-rb, px-rb, and vac-yb were constructed as described (Nelson et al., 2007).

To measure the gravitropic response, seedlings were grown under yellow light for 5 d. After rotating 90° (Figure 1L) or 135° (see Supplemental Figure 3 online) clockwise, the root tip position was recorded with a digital camera once every 2 h for 12 h (Figure 1L) or after 12 h (Supplemental Figure 3 online) and measured using ImageJ. Plants in soil were grown with continuous light in a growth room at 22°C.

Ethyl Methanesulfonate Mutagenesis and Mutant Screen

Approximately 10,000 *DR5rev:GFP* seeds were treated with 0.3% ethyl methanesulfonate for 10 h. After extensive washing, the mutagenized seeds were planted in soil. Approximately 40,000 M2 seeds were germinated on ATS medium. Seedlings with a primary root less than half the length of the control root were transferred to ATS medium supplemented with 75 nM 2,4-D.

After a 12-h treatment, seedlings with reduced levels of GFP signal compared with the control were transferred to soil. Each candidate mutant was crossed to *Col-0 DR5rev:GFP* and *HS:AXR3NT-GUS* lines (Gray et al., 2001). The genetic behavior of each mutant was assessed in the F2 generation. Homozygous F2 plants were backcrossed to *Col-0 DR5rev:GFP* three times prior to analysis.

GUS Histochemical Staining

Six-day-old wild-type and *wxr1* plants homozygous for the *HS:AXR3NT-GUS* were heat shocked for 2 h at 37°C in the dark to induce AXR3NT-GUS expression. Treated seedlings were transferred to control ATS medium \pm 50 nM IAA. At time intervals (0, 20, 40, and 60 min), whole plants were collected and stained overnight at 37°C with staining solution [100 mM Na₂PO₄, pH 7.0, 10 mM EDTA, 0.1% Triton X-100, and 1.0 mM K₃Fe(CN)₆] containing 2 mM X-Gluc to visualize GUS activity. GUS activity was measured in extracts prepared from the terminal 0.5 cm of the root. Dissected tips from \sim 100 roots were homogenized in 100 μ L extraction buffer (50 mM Na₂PO₄, pH 7.0, 10 mM DTT, 1 mM EDTA, 0.1% sodium lauryl sarcosine, and 0.1% Triton X-100). Twenty microliters of

extract were added into 180 μ L MUG assay buffer (1 mM MUG in extraction buffer). After incubation for 4 h at 37°C in the dark, an equal amount of 0.2 M Na_2CO_3 was added to stop the reactions. Enzyme activity in each sample was measured using a spectrofluorimeter. This experiment was repeated three times with the same result.

To examine *BA3:GUS* activity, 6-d-old wild-type and *wxr1* plants carrying the transgene were treated for 12 h on ATS plates with or without 100 nM IAA. Whole plants were stained overnight with X-Gluc staining buffer containing 2 mM X-Gluc. Over 50 roots from *wxr1* and wild-type plants were observed.

Auxin Transport Assay

Auxin transport was assayed using ^3H -IAA radiotracer assays as described (Blakeslee et al., 2007). Seedlings used for transport assays were grown for 5 d at 120 $\mu\text{E}/\text{m}^2\text{s}$ white light, 0.5% sucrose, quarter-strength MS, pH 5.5. Data are from three independent experiments. A 2-mm section centered on the root-shoot transition zone was first excised, followed by an upper hypocotyl section excised immediately below the cotyledon petioles. The root apex was then excised (0.5 mm) followed by serial 2-mm sections up the root. Sampled sections from 10 seedlings were pooled for each measurement and counted in a low-range scintillation counter (Tri-Carb; Perkin-Elmer). Values presented are means and standard deviations from three independent experiments and are presented in order downward from upper hypocotyls to root apex.

IAA Determinations

To measure free auxin levels in aerial tissues (Figure 4I), seedlings were grown on half-strength MS plates (Caisson Laboratories) with 1% sucrose and 0.5% phytigel (Sigma-Aldrich). The Petri dishes were incubated vertically at 22°C for 7 d under continuous light (70 $\mu\text{mol m}^{-2} \text{s}^{-1}$) provided by cool-white fluorescent tubes. Fresh whole seedlings (25 to 50 mg) were harvested, weighed, and frozen in liquid nitrogen. After adding 3 ng of internal standard, [$^{13}\text{C}_6$] IAA, each sample was homogenized in a Mixer-mill (Qiagen) extracted, purified by two sequential solid phase extraction steps, methylated, and then analyzed using selected ion monitoring gas chromatography–mass spectrometry on an Agilent 5973A instrument, exactly as described by Barkawi et al. (2008). At least 10 biological replicates were analyzed for each treatment.

Free IAA determinations in hypocotyl and root segments (Figure 4K) were performed as described (Kim et al., 2007). Seedlings were grown as described for transport assays. Data are from three independent experiments. Results were analyzed for statistical significance in pairwise Student's *t* tests followed by Newman Keuls posthoc analysis.

Microscopy and Drug Treatment

Confocal imaging was performed on an inverted SP/2 confocal microscope (Leica). At least 30 roots were observed for each sample, and each experiment was repeated at least three times. Propidium iodide staining was performed by incubating roots samples in 10 $\mu\text{g}/\text{mL}$ propidium iodide (Sigma-Aldrich) and half-strength MS (1% sucrose) solution for 15 min. For Lugol staining, seedlings were stained in Lugol solution (Sigma-Aldrich; L-6146) for 1 h at room temperature. Immunofluorescence analysis of *Arabidopsis* roots was performed using anti-PIN1 (1:400) and anti-PIN2 (1:800) as described by Dhonukshe et al. (2007). Excitation wavelengths were 488 nm (argon laser); emission was detected at 520 to 560 nm for GFP. Pinhole and gain settings were identical among treatments.

Real-Time RT-PCR Assay

AUX1, *PIN1*, *PIN2*, and *PIN7* levels were determined in root tips of 7-d-old *Col-0* and *wxr1* seedlings grown under yellow light. The terminal 0.5 to 1.0

cm of roots was collected by dissection using a razor blade. Total RNA was isolated from \sim 50 mg of root tips using the RNAeasy plant mini kit (Qiagen). The cDNA was obtained from \sim 2 μg total RNA using a Superscript Double cDNA synthesis kit (Invitrogen). Real-time RT-PCR reactions were performed on a Mastercycler realplex4 (Eppendorf) with 40 cycles of 95°C 15 s, 55°C 10 s, 72°C 20 s. *ACT2* (sense, 5'-ATT-CAGATGCCAGAAAGTCTTGTTTC-3'; antisense, 5'-GCAAGTGCTGTGATTTCTTTGCTCA-3'), *PIN1* (sense, 5'-TGGTCCCTCATTTCCCTCAA-3'; antisense, 5'-GGCAAAGCTGCCTGGATAAT-3'), *PIN2* (sense, 5'-CAA-TAATAGTGTCCGTCGTACCC-3'; antisense, 5'-GCATCGCTTTAGTAGCGAGGTT-3'), *PIN7* (sense, 5'-TTTGGGCTCTTGTGCTTTCA-3'; antisense, 5'-CAGCTTGAACAATGGCCACA-3') and *AUX1* (sense, 5'-GCCTCCGCTCGTCAGAAT-3'; antisense, 5'-ACGGTGGTAAAGCGGAGA-3') primers were synthesized by Sangong Bio-Technologies. SYBR Premix Ex Taq II was ordered from TaKaRa. The real-time RT-PCR experiment was repeated three times using independently isolated RNA samples with similar results.

Light Experiments

Yellow light and UV-deficient conditions were established using Medium Yellow filter 480 (GamProducts) and UV shield filter 1510 (GamProducts) over white fluorescence tube F17T8/TL741 (Philips). Light intensity was measured by a LI-185B Quantum/Radiometer/photometer (LI-COR). The dark treatment involved wrapping plates in aluminum foil. Over 30 roots were measured for each treatment.

Phylogenetic Analysis

An alignment was generated using T-Coffee (Notredame et al., 2000) with the default parameters and adjusted manually in MacClade (Maddison and Maddison, 1989) to remove poorly conserved regions. The phylogeny was inferred with a parallelized version of the MrBayes program (version 3.1.2) using the following parameters: nruns=2 nchains=4 ngen=300000 nst=6 rates=invgamma, samplefreq=100 with burnin=1700. The number of generations was selected using the MCMC convergence diagnostic program AWTY (Nylander et al., 2008). The support values indicate the posterior probabilities based upon the 2600 post-burnin trees in the two runs. The tree was drawn with midpoint rooting using TreeView (Page, 1996) and formatted using OmniGraffle (<http://www.omnigroup.com>).

Accession Numbers

The GenBank accession numbers for the amino acid sequences used in the phylogenetic analysis are as follows: AAO42280, BAD44143, AAD20664, AAP40410, ACI88737, and AAL24114 (*Arabidopsis*); BAD61065, BAD82127, EER92646, CAE02373, BAF15233, and AAV25645 (*Oryza sativa*); EDQ79928, EDQ75723, EDQ71156, EDQ69089, EDQ72935, and EDQ70190 (*Physcomitrella patens*); EEC48020, EEC44574, EEC43483, EEC43518 (*Phaeodactylum tricorutum*); EAL68775 and EAL68330 (*Dictyostelium discoideum*); EAW52119 (*Homo sapiens*); AAF53692 (*Drosophila melanogaster*); and EDQ87821 and EDQ93134 (*Monosiga brevicollis*). The *Phanerochaete chrysosporium* sequence (Phchr1|4271) and the *Volvox carteri* sequences (Volca1|80645, Volca1|90632, Volca1|90737, Volca1|119273, and Volca1|121395) were downloaded from the Department of Energy Joint Genome Institute's websites <http://genome.jgi-psf.org/Phchr1> and <http://genome.jgi-psf.org/Volca1>. The *Cyanidioschyzon merolae* sequences (CMI082C, CMI124C, CMM174C, CMN030C, CMP326C, CMQ317C, and CMR069C) were downloaded from <http://merolae.biol.s.u-tokyo.ac.jp/>. The *Arabidopsis* Genome Initiative locus number for the major genes discussed in this article are as follows: *RUS2/WXR1* (at2g31190), *TIR1* (at3g62980), *AFB1* (at4g03190), *AFB2* (at3g26810), *AFB3* (at1g12820), *AXR2/IAA7* (at3g23050), *ABC1/PGP1* (at2g36910), *PIN1* (at1g73590), *PIN2* (at5g57090), *PIN7*

(at1g23080), *AUX1* (at2g38120), *VHA-A1* (at2g28520), *ARA7* (at4g19640), and *GNOM* (at1g13980).

Supplemental Data

The following materials are available in the online version of this article.

Supplemental Figure 1. NAA and IAA Response in *DR5rev:GFP* and *DR5rev:GFPwrx1* Plants.

Supplemental Figure 2. Effect of Light Wavelength on *wrx1* Root Growth.

Supplemental Figure 3. The *wrx1* Mutation Enhances the Gravitropic Defect Observed in the *aux1*, *pgp1*, and *axr2* Mutants.

Supplemental Figure 4. Levels of the Tonoplast Marker vac-yb Is Slightly Increased in *wrx1* Plants.

Supplemental Figure 5. WXR1 Is a Member of the DUF647 Family.

Supplemental Figure 6. The DUF647 Protein Family Diverged Early in Eukaryote Evolution.

Supplemental Figure 7. WXR1 Is Expressed in All Organs in *Arabidopsis*.

Supplemental Figure 8. Growth of *wrx1* Seedlings in UV-Deficient Light.

Supplemental Data Set 1. Text File of the Alignment Used for the Phylogenetic Analysis Shown in Supplemental Figure 6.

ACKNOWLEDGMENTS

Work in the authors' labs was supported by grants from the National Institutes of Health (GM43644 to M.E.), the National Science Foundation (MCB0725149 and DBI-PGRP-0606666 to J.D.C.), and the USDA (National Research Initiative, 2005-35318-16197, to J.D.C.).

Received January 21, 2010; revised May 12, 2010; accepted June 2, 2010; published June 18, 2010.

REFERENCES

- Abas, L., Benjamins, R., Malenica, N., Paciorek, T., Wisniewska, J., Moulinier-Anzola, J.C., Sieberer, T., Friml, J., and Luschnig, C. (2006). Intracellular trafficking and proteolysis of the *Arabidopsis* auxin-efflux facilitator PIN2 are involved in root gravitropism. *Nat. Cell Biol.* **8**: 249–256.
- Bandyopadhyay, A., et al. (2007). Interactions of PIN and PGP auxin transport mechanisms. *Biochem. Soc. Trans.* **35**: 137–141.
- Barkawi, L.S., Tam, Y.Y., Tillman, J.A., Pederson, B., Calio, J., Al-Amier, H., Emerick, M., Normanly, J., and Cohen, J.D. (2008). A high-throughput method for the quantitative analysis of indole-3-acetic acid and other auxins from plant tissue. *Anal. Biochem.* **372**: 177–188.
- Benjamins, R., and Scheres, B. (2008). Auxin: The looping star in plant development. *Annu. Rev. Plant Biol.* **59**: 443–465.
- Benkova, E., Michniewicz, M., Sauer, M., Teichmann, T., Seifertova, D., Jurgens, G., and Friml, J. (2003). Local, efflux-dependent auxin gradients as a common module for plant organ formation. *Cell* **115**: 591–602.
- Blakeslee, J.J., et al. (2007). Interactions among PIN-FORMED and P-glycoprotein auxin transporters in *Arabidopsis*. *Plant Cell* **19**: 131–147.
- Blilou, I., Xu, J., Wildwater, M., Willemsen, V., Paponov, I., Friml, J., Heidstra, R., Aida, M., Palme, K., and Scheres, B. (2005). The PIN auxin efflux facilitator network controls growth and patterning in *Arabidopsis* roots. *Nature* **433**: 39–44.
- Davies, P.J. (1995). The plant hormones: Their nature, occurrence and functions. In *Plant Hormones Physiology, Biochemistry and Molecular Biology*, P.J. Davies, ed (Dordrecht, The Netherlands: Kluwer Academic Publishers), pp. 1–12.
- Dettmer, J., Hong-Hermesdorf, A., Stierhof, Y.D., and Schumacher, K. (2006). Vacuolar H⁺-ATPase activity is required for endocytic and secretory trafficking in *Arabidopsis*. *Plant Cell* **18**: 715–730.
- Dharmasiri, N., Dharmasiri, S., and Estelle, M. (2005a). The F-box protein TIR1 is an auxin receptor. *Nature* **435**: 441–445.
- Dharmasiri, N., Dharmasiri, S., Weijers, D., Lechner, E., Yamada, M., Hobbie, L., Ehrismann, J.S., Jurgens, G., and Estelle, M. (2005b). Plant development is regulated by a family of auxin receptor F box proteins. *Dev. Cell* **9**: 109–119.
- Dharmasiri, S., Swarup, R., Mockaitis, K., Dharmasiri, N., Singh, S.K., Kowalchuk, M., Marchant, A., Mills, S., Sandberg, G., Bennett, M.J., and Estelle, M. (2006). AXR4 is required for localization of the auxin influx facilitator AUX1. *Science* **312**: 1218–1220.
- Dhonukshe, P., Aniento, F., Hwang, I., Robinson, D.G., Mravec, J., Stierhof, Y.D., and Friml, J. (2007). Clathrin-mediated constitutive endocytosis of PIN auxin efflux carriers in *Arabidopsis*. *Curr. Biol.* **17**: 520–527.
- Dhonukshe, P., et al. (2008). Generation of cell polarity in plants links endocytosis, auxin distribution and cell fate decisions. *Nature* **456**: 962–966.
- Dunkley, T.P., et al. (2006). Mapping the *Arabidopsis* organelle proteome. *Proc. Natl. Acad. Sci. USA* **103**: 6518–6523.
- Ferro, M., Salvi, D., Brugiere, S., Miras, S., Kowalski, S., Louwagie, M., Garin, J., Joyard, J., and Rolland, N. (2003). Proteomics of the chloroplast envelope membranes from *Arabidopsis thaliana*. *Mol. Cell. Proteomics* **2**: 325–345.
- Friml, J., Benkova, E., Blilou, I., Wisniewska, J., Hamann, T., Ljung, K., Woody, S., Sandberg, G., Scheres, B., Jurgens, G., and Palme, K. (2002a). AtPIN4 mediates sink-driven auxin gradients and root patterning in *Arabidopsis*. *Cell* **108**: 661–673.
- Friml, J., Wisniewska, J., Benkova, E., Mendgen, K., and Palme, K. (2002b). Lateral relocation of auxin efflux regulator PIN3 mediates tropism in *Arabidopsis*. *Nature* **415**: 806–809.
- Friml, J., et al. (2004). A PINOID-dependent binary switch in apical-basal PIN polar targeting directs auxin efflux. *Science* **306**: 862–865.
- Gälweiler, L., Guan, C., Müller, A., Wisman, E., Mendgen, K., Yephremov, A., and Palme, K. (1998). Regulation of polar auxin transport by AtPIN1 in *Arabidopsis* vascular tissue. *Science* **282**: 2226–2230.
- Geisler, M., et al. (2005). Cellular efflux of auxin catalyzed by the *Arabidopsis* MDR/PGP transporter AtPGP1. *Plant J.* **44**: 179–194.
- Geldner, N., Anders, N., Wolters, H., Keicher, J., Kornberger, W., Müller, P., Delbarre, A., Ueda, T., Nakano, A., and Jurgens, G. (2003). The *Arabidopsis* GNOM ARF-GEF mediates endosomal recycling, auxin transport, and auxin-dependent plant growth. *Cell* **112**: 219–230.
- Geldner, N., Friml, J., Stierhof, Y.D., Jurgens, G., and Palme, K. (2001). Auxin transport inhibitors block PIN1 cycling and vesicle trafficking. *Nature* **413**: 425–428.
- Gil, P., Dewey, E., Friml, J., Zhao, Y., Snowden, K.C., Putterill, J., Palme, K., Estelle, M., and Chory, J. (2001). BIG: A calossin-like protein required for polar auxin transport in *Arabidopsis*. *Genes Dev.* **15**: 1985–1997.
- Gray, W.M., Kepinski, S., Rouse, D., Leyser, O., and Estelle, M.

- (2001). Auxin regulates SCFTIR1-dependent degradation of AUX/IAA proteins. *Nature* **414**: 271–276.
- Gray, W.M., Ostin, A., Sandberg, G., Romano, C.P., and Estelle, M.** (1998). High temperature promotes auxin-mediated hypocotyl elongation in *Arabidopsis*. *Proc. Natl. Acad. Sci. USA* **95**: 7197–7202.
- Grieneisen, V.A., Xu, J., Maree, A.F., Hogeweg, P., and Scheres, B.** (2007). Auxin transport is sufficient to generate a maximum and gradient guiding root growth. *Nature* **449**: 1008–1013.
- Hamann, T., Mayer, U., and Jurgens, G.** (1999). The auxin-insensitive bodenlos mutation affects primary root formation and apical-basal patterning in the *Arabidopsis* embryo. *Development* **126**: 1387–1395.
- Jaillais, Y., Fobis-Loisy, I., Miede, C., Rollin, C., and Gaude, T.** (2006). AtSNX1 defines an endosome for auxin-carrier trafficking in *Arabidopsis*. *Nature* **443**: 106–109.
- Jaillais, Y., Santambrogio, M., Rozier, F., Fobis-Loisy, I., Miede, C., and Gaude, T.** (2007). The retromer protein VPS29 links cell polarity and organ initiation in plants. *Cell* **130**: 1057–1070.
- Kepinski, S., and Leyser, O.** (2005). The *Arabidopsis* F-box protein TIR1 is an auxin receptor. *Nature* **435**: 446–451.
- Kim, J.I., et al.** (2007). *yucca6*, a dominant mutation in *Arabidopsis*, affects auxin accumulation and auxin-related phenotypes. *Plant Physiol.* **145**: 722–735.
- Kleine-Vehn, J., Huang, F., Naramoto, S., Zhang, J., Michniewicz, M., Offringa, R., and Friml, J.** (2009). PIN auxin efflux carrier polarity is regulated by PINOID kinase-mediated recruitment into GNOM-independent trafficking in *Arabidopsis*. *Plant Cell* **21**: 3839–3849.
- Kleine-Vehn, J., Leitner, J., Zwiewka, M., Sauer, M., Abas, L., Luschnig, C., and Friml, J.** (2008). Differential degradation of PIN2 auxin efflux carrier by retromer-dependent vacuolar targeting. *Proc. Natl. Acad. Sci. USA* **105**: 17812–17817.
- Laxmi, A., Pan, J., Morsy, M., and Chen, R.** (2008). Light plays an essential role in intracellular distribution of auxin efflux carrier PIN2 in *Arabidopsis thaliana*. *PLoS One* **3**: e1510.
- Leasure, C.D., Tong, H., Yuen, G., Hou, X., Sun, X., and He, Z.H.** (2009). ROOT UV-B sensitive2 acts with root UV-B sensitive1 in a root ultraviolet B-sensing pathway. *Plant Physiol.* **150**: 1902–1915.
- Lee, G.J., Sohn, E.J., Lee, M.H., and Hwang, I.** (2004). The *Arabidopsis* rab5 homologs rha1 and ara7 localize to the prevacuolar compartment. *Plant Cell Physiol.* **45**: 1211–1220.
- Lincoln, C., Britton, J.H., and Estelle, M.** (1990). Growth and development of the *axr1* mutants of *Arabidopsis*. *Plant Cell* **2**: 1071–1080.
- Maddison, W.P., and Maddison, D.R.** (1989). Interactive analysis of phylogeny and character evolution using the computer program MacClade. *Folia Primatol. (Basel)* **53**: 190–202.
- Marchant, A., Kargul, J., May, S.T., Muller, P., Delbarre, A., Perrot-Rechenmann, C., and Bennett, M.J.** (1999). AUX1 regulates root gravitropism in *Arabidopsis* by facilitating auxin uptake within root apical tissues. *EMBO J.* **18**: 2066–2073.
- Michniewicz, M., et al.** (2007). Antagonistic regulation of PIN phosphorylation by PP2A and PINOID directs auxin flux. *Cell* **130**: 1044–1056.
- Mockaitis, K., and Estelle, M.** (2008). Auxin receptors and plant development: A new signaling paradigm. *Annu. Rev. Cell Dev. Biol.* **24**: 55–80.
- Nelson, B.K., Cai, X., and Nebenfuhr, A.** (2007). A multicolored set of in vivo organelle markers for co-localization studies in *Arabidopsis* and other plants. *Plant J.* **51**: 1126–1136.
- Noh, B., Bandyopadhyay, A., Peer, W.A., Spalding, E.P., and Murphy, A.S.** (2003). Enhanced gravi- and phototropism in plant *mdr* mutants mislocalizing the auxin efflux protein PIN1. *Nature* **423**: 999–1002.
- Noh, B., Murphy, A.S., and Spalding, E.P.** (2001). Multidrug resistance-like genes of *Arabidopsis* required for auxin transport and auxin-mediated development. *Plant Cell* **13**: 2441–2454.
- Notredame, C., Higgins, D.G., and Heringa, J.** (2000). T-Coffee: A novel method for fast and accurate multiple sequence alignment. *J. Mol. Biol.* **302**: 205–217.
- Nylander, J.A., Wilgenbusch, J.C., Warren, D.L., and Swofford, D.L.** (2008). AWTY (are we there yet?): A system for graphical exploration of MCMC convergence in Bayesian phylogenetics. *Bioinformatics* **24**: 581–583.
- Oono, Y., Chen, Q.G., Overvoorde, P.J., Kohler, C., and Theologis, A.** (1998). age mutants of *Arabidopsis* exhibit altered auxin-regulated gene expression. *Plant Cell* **10**: 1649–1662.
- Paciorek, T., Zazimalova, E., Ruthardt, N., Petrasek, J., Stierhof, Y.D., Kleine-Vehn, J., Morris, D.A., Emans, N., Jurgens, G., Geldner, N., and Friml, J.** (2005). Auxin inhibits endocytosis and promotes its own efflux from cells. *Nature* **435**: 1251–1256.
- Page, R.D.** (1996). TreeView: An application to display phylogenetic trees on personal computers. *Comput. Appl. Biosci.* **12**: 357–358.
- Pan, J., Fujioka, S., Peng, J., Chen, J., Li, G., and Chen, R.** (2009). The E3 ubiquitin ligase SCFTIR1/AFB and membrane sterols play key roles in auxin regulation of endocytosis, recycling, and plasma membrane accumulation of the auxin efflux transporter PIN2 in *Arabidopsis thaliana*. *Plant Cell* **21**: 568–580.
- Petrasek, J., and Friml, J.** (2009). Auxin transport routes in plant development. *Development* **136**: 2675–2688.
- Pickett, F.B., Wilson, A.K., and Estelle, M.** (1990). The *aux1* mutation of *Arabidopsis* confers both auxin and ethylene resistance. *Plant Physiol.* **94**: 1462–1466.
- Robert, H.S., and Friml, J.** (2009). Auxin and other signals on the move in plants. *Nat. Chem. Biol.* **5**: 325–332.
- Sabatini, S., Beis, D., Wolkenfelt, H., Murfett, J., Guilfoyle, T., Malamy, J., Benfey, P., Leyser, O., Bechtold, N., Weisbeek, P., and Scheres, B.** (1999). An auxin-dependent distal organizer of pattern and polarity in the *Arabidopsis* root. *Cell* **99**: 463–472.
- Sukumar, P., Edwards, K.S., Rahman, A., Delong, A., and Muday, G.K.** (2009). PINOID kinase regulates root gravitropism through modulation of PIN2-dependent basipetal auxin transport in *Arabidopsis*. *Plant Physiol.* **150**: 722–735.
- Swarup, R., Friml, J., Marchant, A., Ljung, K., Sandberg, G., Palme, K., and Bennett, M.** (2001). Localization of the auxin permease AUX1 suggests two functionally distinct hormone transport pathways operate in the *Arabidopsis* root apex. *Genes Dev.* **15**: 2648–2653.
- Swarup, R., et al.** (2004). Structure-function analysis of the presumptive *Arabidopsis* auxin permease AUX1. *Plant Cell* **16**: 3069–3083.
- Tao, Y., et al.** (2008). Rapid synthesis of auxin via a new tryptophan-dependent pathway is required for shade avoidance in plants. *Cell* **133**: 164–176.
- Tong, H., Leasure, C.D., Hou, X., Yuen, G., Briggs, W., and He, Z.H.** (2008). Role of root UV-B sensing in *Arabidopsis* early seedling development. *Proc. Natl. Acad. Sci. USA* **105**: 21039–21044.
- Wilson, A.K., Pickett, F.B., Turner, J.C., and Estelle, M.** (1990). A dominant mutation in *Arabidopsis* confers resistance to auxin, ethylene and abscisic acid. *Mol. Gen. Genet.* **222**: 377–383.
- Wisniewska, J., Xu, J., Seifertova, D., Brewer, P.B., Ruzicka, K., Bliou, I., Rouquie, D., Benkova, E., Scheres, B., and Friml, J.** (2006). Polar PIN localization directs auxin flow in plants. *Science* **312**: 883.
- Zhang, J., Nodzynski, T., Pencik, A., Rolcik, J., and Friml, J.** (2010). PIN phosphorylation is sufficient to mediate PIN polarity and direct auxin transport. *Proc. Natl. Acad. Sci. USA* **107**: 918–922.